Cristian Villa-Pérez, Isabel C. Ortega, Angélica M. Payán-Aristizábal, Gustavo Echeverría, Gloria C. Valencia-Uribe and Delia B. Soria*

Synthesis, crystal structure and physicochemical characterization of a Hg(II) complex with 6-methoxyquinoline as ligand

DOI 10.1515/znb-2015-0069
Received April 7, 2015; accepted May 5, 2015

Abstract: A new complex of Hg(II) with 6-methoxyquinoline ($C_{10}H_9NO$-6MQ) has been synthesized and characterized. The structure of the complex $Hg(6MQ)Cl_2$ was determined by single crystal X-ray diffraction. It crystallizes in the monoclinic space group $P2_1/c$ with a = 3.9139(3), b = 26.3400(2), c = 10.9090(9) Å, β = 89.833(6)°, V = 1124.6(1) Å^3 and Z = 4 molecules per unit cell. The coordination geometry of the mercury(II) center can be described as a distorted square pyramid formed by one nitrogen atom of the 6MQ and four chlorine atoms. Fourier transform infrared, Raman and UV/Vis spectroscopic studies have been carried out to characterize the compound, using theoretical calculations for the assignment of the experimentally observed bands. The thermal behavior was investigated by thermogravimetric analysis. The quantum yield of singlet molecular oxygen production Φ_Δ was measured with steady-state methods in ethanol, using 9,10-dimethylanthracene (DMA) as actinometer and Bengal rose as reference photosensitizer. The resultant singlet molecular oxygen was detected indirectly by photooxidation reactions of DMA. The luminescence properties have also been studied.

***Corresponding author: Delia B. Soria,** CEQUINOR (CONICET, CCT-La Plata), Facultad de Ciencias Exactas, Departamento de Química, Universidad Nacional de la Plata, 47 y 115 (1900) La Plata, Argentina, Fax: +54 221 4240172, E-mail: soria@quimica.unlp.edu.ar
Cristian Villa-Pérez: CEQUINOR (CONICET, CCT-La Plata), Facultad de Ciencias Exactas, Departamento de Química, Universidad Nacional de la Plata, 47 y 115 (1900) La Plata, Argentina
Isabel C. Ortega, Angélica M. Payán-Aristizábal and Gloria C. Valencia-Uribe: GIAFOT, Facultad de Ciencias, Departamento de Química, Universidad Nacional de Colombia-Sede Medellín, Calle 59 A No. 63-020, Medellín, Colombia
Gustavo Echeverría: Facultad de Ciencias Exactas, Departamento de Física, Universidad Nacional de La Plata and IFLP (CONICET, CCT-La Plata), C.C. 67, 1900 La Plata, Argentina

Keywords: density functional calculations; Hg(II) complex; 6-methoxyquinoline; singlet oxygen; spectroscopic properties; X-ray structure.

1 Introduction

The photosensitizing properties of some alkaloids including quinine (Q) and primaquine (PQ) were reported in the last years of the 19th century. The study of their physicochemical properties including the photochemical behavior was accelerated in the beginning of the 20th century due to their wider use as drugs against malaria and their phototoxic side effects [1, 2].

Figure 1 shows the Q and PQ formulae containing the 6-methoxyquinolinyl rest. The 6-methoxyquinolinyl group has been associated with the phototoxic side effects of these drugs due to its elevated quantum yield of singlet molecular oxygen (O_2 ($^1\Delta_g$)) production of 0.96 ± 0.08 when perinaphtenone was used as reference [3]. This value indicates the high phototoxicity of the 6-methoxyquinolinyl rest. Due to this it could be used in advanced oxidation processes (AOP), because O_2 ($^1\Delta_g$) is able to attack organic molecules and microorganisms [4].

Because 6-methoxyquinoline (6MQ) is a liquid compound that is easily oxidizable, the primary objective of this paper was to study its behavior in the solid state. For that reason and considering the small number of complexes with 6MQ as ligand in the literature [5], we are interested in the study of its solid metal complexes. It is well known that mercury(II) has potential as a poison or as a medicine due to its interference in biological systems. These properties make it especially interesting for studying its coordination properties. A few Hg complexes are still used in medical treatments as antiseptic, even though it is known that this cation has potentially toxic side effects [6]. In view of the need to know about the Hg complexes and in order to improve the 6MQ properties, here we describe the synthesis of a novel Hg(II) complex. The crystal structure, spectroscopic properties, quantum yield

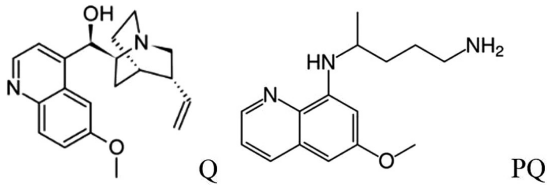

Fig. 1: Molecular formulae of quinine (Q) and primaquine (PQ) containing the 6MQ moiety.

of $^1O_2$ generation and the luminescence were studied. The assignment of experimental infrared bands was accomplished with the aid of theoretical results based on density functional theory (DFT). The thermogravimetric (TG) analysis was also carried out and the results discussed.

2 Experimental section

2.1 Equipment and methods

The Fourier transform infrared (FTIR) spectra were obtained with a Bruker EQUINOX 55 spectrophotometer (Billerica, MA, USA), in the range from 4000 to 400 cm^{-1}, using the KBr pellets for the solid complex and KBr windows for the liquid ligand, with a spectral resolution of 4 cm^{-1}. The far FTIR spectrum of the complex was measured with the aid of a Nicolet Magna instrument (Waltham, MA, USA) equipped with a deuterated triglycine sulfate detector, in the 400 to 50 cm^{-1} spectral range, using a polyethylene pellet. The Raman spectra of the 6MQ and the complex were measured in the 1000–80 cm^{-1} spectral range using a Horiba-Jobin-Yvon (Kyoto, Japan) T64000 Raman spectrometer, with a confocal microscope and charge-coupled device (CCD) detection. Excitation radiation of 514.5 nm (argon laser) for the ligand and 647.1 nm (krypton laser) for the complex were used. Both spectra were recorded at different excitation levels due to the strong fluorescence of the complex (see Section 3.4 below). TG analysis was performed using a TA Instrument (New Castle, DE, USA) 2950 unit at a heating rate of 5 °C min^{-1} and a nitrogen flow of 50 mL min^{-1}. The electronic absorption spectrum of the complex was measured on freshly prepared ethanol solution (~10^{-4} M) in the 190–1100 nm spectral range, with the help of a PerkinElmer (Waltham, MA, USA) Lambda 35 spectrophotometer, using a 10 mm quartz cell. The quantum yield of singlet oxygen ($O_2(^1\Delta_g)$) generation was measured indirectly in steady state at 25 °C and irradiating the sample with a UV light source centered at 350 nm. The emission spectrum of an ethanolic solution (~10^{-4} M) was recorded using a PerkinElmer LS 50B spectrofluorometer.

2.2 Synthesis of $Hg6MQCl_2$

The 6MQ ligand was purchased from Sigma Aldrich (St. Louis, MO, USA) and purified by reduced pressure distillation. The complex was prepared adding liquid 6MQ to an ethanolic solution containing $HgCl_2$ in 2:1 stoichiometric ratio. Then, the resulting white solid was separated by filtration. The slow evaporation of an ethanolic colorless solution provided well-developed white crystals that were suitable for X-ray diffraction. The yield was 87 %.

2.3 X-ray structure determination

The intensity data for the complex were collected on an Agilent Gemini Diffractometer equipped with an EOS CCD detector with graphite-monochromatized MoK_α radiation (λ = 0.71073 Å). X-ray diffraction intensities were collected (ω scans with θ and κ offsets), integrated and scaled with the CrysAlisPro (Agilent Technologies Ltd., Yarnton, Oxfordshire, UK) [7] suite of programs. The unit cell parameters were obtained by least-squares refinement based on the angular settings of all collected reflections with intensities larger than seven times the standard deviation. Data were corrected empirically for absorption employing the multi-scan method implemented in Crys AlisPro. The structure was solved by Direct Methods with Shelxs-97 (Göttingen, Lower Saxony, Germany) [8, 9] and the molecular model refined by a full-matrix least-squares procedure on F^2 with Shelxl-97 [9, 10]. The hydrogen atoms were positioned stereochemically and refined with the riding model. Crystal data, data collection and refinement parameters are summarized in Table 1.

CCDC 1034690 contains the supplementary crystallographic data for this paper. These data can be obtained free of charge from The Cambridge Crystallographic Data Centre via www.ccdc.cam.ac.uk/data_request/cif.

2.4 Computational methods

The computational studies of the complex and the free ligand were performed using the DFT implemented in Gaussian 03 (Wallingford, CT, USA) [11].

The systems studied herein were subjected to energy minimizations using the B3LYP [12] functional with the 6-31 + G** basis set [13] for the non-metal atoms and the Los Alamos effective core potentials LANL2DZ [14–16] for the metal. The vibrational frequencies for the compounds were calculated in gas phase using the second derivatives. On this basis, the vibrational modes have been assigned using 0.97 as scaling factor.

Table 1: Crystal data and numbers pertinent to data collection and structure refinement for the complex $Hg(6MQ)Cl_2$.

Empiric formula	$HgC_{10}H_9NOCl_2$
Formula weight	430.68
Temperature, K	293
Wavelength, Å	0.71073
Crystal system	monoclinic
Space group	$P2_1/c$
Unit cell dimensions	
a, Å	3.9139(3)
b, Å	26.340(2)
c, Å	10.9090(9)
β, deg	89.833(6)
Volume, Å^3	1124.6(1)
Z/Density (calcd.), g cm^{-3}	4/2.54
Absorption coefficient	14.1 mm^{-1}
F(000), e	792
Index ranges	$-4 \le h \le 5$
	$-35 \le k \le 15$
	$-13 \le l \le 13$
θ range data collection, deg	3.61–29.41
Refl. collected/unique/R_{int}	4576/2597/0.0339
Refl. with $I > 2\sigma(I)$	2156
Completeness to $\theta = 29.41°$, %	99.53
Absorption correction	Multi-scan (AbsPack in CrysAlisPro [7])
Maximum/minimum transmission	1.000/0.837
Refinement method	Full-matrix least-squares on F^2
Data/ref. parameters	2597/136
Final $R1/wR2$ [$I > 2\sigma(I)$]	0.0523/0.1165
Final $R1/wR2$ (all data)	0.0677/0.1242
Goodness of fit on F^2	1.204
Largest diff. peak/hole, e Å^{-3}	1.713/−1.609

Table 2: Selected bond lengths (Å) and angles (deg) observed and calculated.[a]

	Experimental	B3LYP
Distances		
Hg1–N1	2.474(9)	2.536
Hg1–Cl1	2.347(3)	2.460
Hg1–Cl2	2.357(3)	2.470
Hg1–Cl1^{iii}	3.130(3)	
Hg1–Cl2^{ii}	3.023(3)	
Angles		
Cl1–Hg1–N1	98.9(2)	111.6
Cl2–Hg1–N1	97.0(2)	97.1
Cl1–Hg1–Cl2	164.14(1)	151.27
N1–Hg1–Cl2^{ii}	87.9(2)	
N1–Hg1–Cl1^{iii}	104.1(2)	
Cl1–Hg1–Cl2^{ii}	88.44(9)	
Cl1–Hg1–Cl1^{iii}	90.04(9)	
Cl2–Hg1–Cl2^{ii}	92.50(9)	
Cl2–Hg1–Cl1^{iii}	85.76(9)	

[a]For symmetry operations, see Fig. 2.

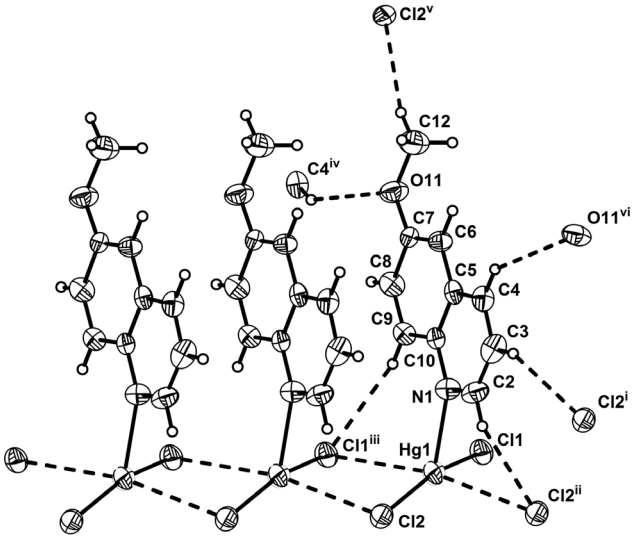

Fig. 2: Part of the crystal structure of $Hg(6MQ)Cl_2$ showing the infinite $HgCl_2$ chains and the weak intermolecular C–H···O/Cl interactions (denoted by dashed lines) with crystallographic labeling of the non-H atoms. Displacement ellipsoids for non-H atoms are drawn at the 50 % probability level. Crystal symmetry operations: (i) $-x, -y, -z$; (ii) $x + 1, y, z$; (iii) $x - 1, y, z$; (iv) $-1 + x, -1/2 - y, 1/2 + z$; (v) $-x - 1, y - 1/2, -z + 1/2$; (vi) $x + 1, -y - 1/2, z - 1/2$.

3 Results and discussion

3.1 Crystal and molecular structure of the complex

Only a few complexes with 6MQ as ligand have been studied as powders, and their structures were not reported. Here we describe the crystal structure of a Hg(II) complex with 6MQ as ligand. This information is useful in order to shed light on the coordinative properties of the ligand which has not previously been reported. Table 2 lists selected experimental and calculated (B3LYP) bond distances and angles around the Hg(II) cation. Figure 2 shows the coordination sphere of the metal center bonded to a 6MQ molecule along with the labeling scheme. The coordination sphere of each Hg(II) cation consists of one 6MQ nitrogen atom at a Hg–N distance of 2.474(9) Å, two chlorine atoms forming two strong Hg–Cl bonds (2.346(3) and 2.341(3) Å) and two weak intermolecular Hg···Cl interactions at 3.025(4) and 3.125(4) Å, completing in this way a distorted square pyramidal geometry. The Hg–Cl bond lengths are in agreement with those reported for similar complexes with quinolinic ligands [17–19]. Adjacent mercury cations are bridged by two chlorine atoms forming infinite linear chains parallel to the crystallographic a axis (hereafter called $HgCl_2$ chain). The $HgCl_2$ chain could be described

as an infinite chain of distorted mercury square pyramids that share edges; see Fig. 2. The Hg···Hg distance along the chain is 3.9139(6) Å, longer than the sum of van der Waals radii (3.50(7) Å) [20] but very close to that found in similar complexes with weak mercury interactions [17–19]. The $HgCl_2$ chains are also supported by weak hydrogen bond interactions between two quinolinic carbon atoms and two Cl atoms, bonded to the adjacent Hg cations (C2–H2···Cl2^{ii} and C9–H9···Cl1^{iii}). They are depicted in dashed lines in Fig. 2, and their characteristic parameters are listed in Table 3. The 6MQ molecules, which coordinate to the metal center, are arranged in a face-to-face offset stacking along the crystallographic *a* axis at a ring plane distance of 3.491 Å. The short distance of the π–π planes is an important criterion to suggest an intermolecular $\pi\cdots\pi$ interaction between quinolinic rings; see Fig. 2. Similar $\pi\cdots\pi$ interactions have been found in complexes of other heteroaromatic ligands containing nitrogen [17, 21, 22].

Several polymeric mercury compounds ($[HgCl_2(bpym)]_n$, $[Hg_2Br_4(bpym)]_n$ (bpym = 5,5′-bipyrimidine) and $[HgX_2(2,2'\text{-bipyrazine})]_n$ (X = Cl and Br)) have been studied [17]. In those complexes the halide bridging interactions are not sufficient to induce the linearity of the mercury atoms. However, the packing of the $HgCl_2$ chains in those complexes is strongly influenced by the $\pi\cdots\pi$ interaction of the rings [17]. In $Hg(6MQ)Cl_2$ the square pyramids of the nearest adjacent chains are placed at a distance of 4.1389(1) Å with their square bases arranged in the opposite way. Due to this arrangement, the Cl1 atom of one mercury chain is situated at a Hg···Cl1^{i} distance of 3.4118(2) Å from the other one. This distance is greater than the mean value of the Hg–Cl distances, and thus no octahedral geometry is established.

In addition, the $Hg(6MQ)Cl_2$ chains are linked by weak intermolecular C–H···O/Cl hydrogen bond interactions stabilizing the three-dimensional crystal structure (see Fig. 2 and Table 3).

The geometry of the Hg complex has also been optimized at the B3LYP level. The gas phase optimization rendered a structure slightly different from the experimentally determined one (Table 2). The optimization resulted in the trigonal coordination sphere around the Hg(II) cation with one 6MQ nitrogen atom at 2.536 Å Hg–N distance and two chlorine atoms at 2.460 and 2.470 Å Hg–Cl distances. The optimized geometry is in a good agreement with the experimental one found by X-Ray diffraction taking into account that the DFT calculation is performed in vacuum and so ignores the weak Hg···Cl interactions found in the solid state (see Fig. 2).

Table 3: Hydrogen bond distances and angles for $Hg(6MQ)Cl_2$ (Å and deg).[a]

D–H···A	D–H	H···A	D···A	D–H···A
C3–H3···Cl2^{i}	0.93	2.91	3.74(1)	149.2
C2–H2···Cl2^{ii}	0.93	2.97	3.60(1)	125.5
C9–H9···Cl1^{iii}	0.93	2.90	3.79(1)	159.9
C12–H12A···Cl2^{v}	0.96	3.00	3.94(1)	167.9
C4–H4···O11^{vi}	0.93	2.71	3.49(1)	142.1

[a]For symmetry operations, see Fig. 2.

3.2 Vibrational spectra

The FTIR spectrum of $Hg(6MQ)Cl_2$ was compared with that of the free 6MQ. Both spectra are shown in Fig. 3. Table 4 shows the experimental and theoretical vibrational frequencies and their respective assignments. The agreement between the experimental and calculated IR frequencies is good.

In the ligand spectrum the bands due to the aliphatic and aromatic C–H groups are observed in the 3100–2800 cm^{-1} region. These bands were shifted to lower frequencies upon complexation. This fact is in agreement with X-ray diffraction evidence that four quinolinic carbon atoms are involved as hydrogen donors in the weak intermolecular hydrogen bonding (Section 3.1). In the ligand spectrum the bands assigned to ring vibrations (1623, 1572 and 1500 cm^{-1}) were shifted to higher wavenumber in the complex spectrum indicating binding of the mercury to the nitrogen atom of the quinolinic ring.

The slight change observed in the ν (C–O) vibration (from 1230 to 1233 cm^{-1}) after coordination is probably due

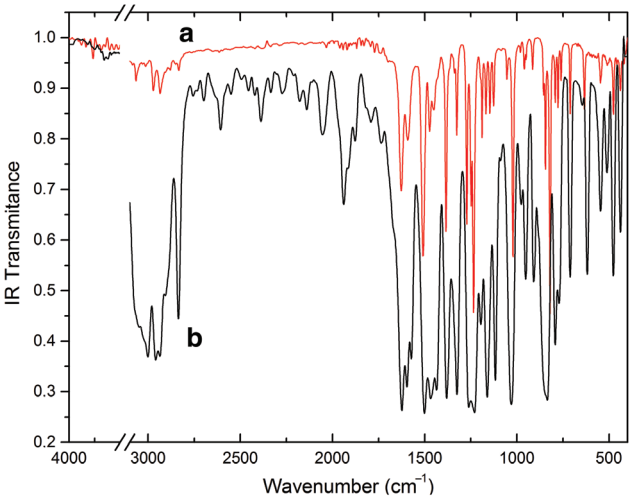

Fig. 3: FTIR spectra of (a) the solid complex $Hg(6MQ)Cl_2$ and (b) the liquid ligand 6MQ (in uncomplexed form).

Table 4: Observed and calculated FTIR frequencies (cm^{-1}) for the 6MQ ligand and the complex $Hg(6MQ)Cl_2$.

Ligand		Complex		Assignments
Observed	B3LYP	Observed	B3LYP	
3075 s	3143 (11)	3066 w	3127 (9)	ν C–H
3025 s	3125 (32)	3014 vw	3123 (10)	ν C–H
3001 s	3120 (9.8)	3000 sh	3109 (13)	ν C–H
2958 s	3102 (24)	2971 w	3096 (7.4)	ν C–H
2935 s	3096 (1.7)	2935 w	3093 (15)	ν C–H
2905 s	3086 (18)	2905 sh	3067 (21)	ν_{as} C–H_3
2887 s	3016 (38)	2880 vw	2996 (35)	ν_{as} C–H_3
2835 vs	2944 (62)	2834 vw	2933 (46)	ν_s C–H_3
1623 vs	1624 (77)	1627 s	1627 (105)	Ring
1572 s	1548 (27)	1593 m	1578 (11)	Ring
1502 vs	1503 (82)	1510 vs	1511 (119)	Ring + δ C=N–C
1468 s	1469 (15)	1471 m	1470 (34)	δ C–H_3
		1451 w	1457 (7)	δ C–H_3
1436 s	1445 (1.7)			Ring
1381 vs	1380 (4.8)	1384 s	1375 (94)	Ring
1325 s	1330 (22)	1327 m	1339 (13)	Ring + ν_{as} C=N–C
1261 vs	1268 (28)	1271 s	1274 (135)	Ring
1230 vs	1233 (12)	1233 vs	1233 (12)	ν C–O
1196 s	1171 (49)	1191 m	1193 (39)	ρ C–H_3 + ν C–O
1161 s	1164 (36)	1168 m	1168 (17)	ρ C–H_3
1117 s	1120 (0.5)	1126 w	1120 (19)	Ring δ C–O
		1052 vw	1050 (15)	Ring
1030 vs	1031 (3.7)	1022 s	1036 (55)	ν H_3C–O
952 s	948 (0.5)	957 vw	958 (0.1)	Ring
909 s	881 (51)	915 vw	905 (14)	δ (C=N–C)
		847 s	842 (65)	Ring
835 s	835 (54)	821 vs	841 (5.1)	Ring
792 s	793 (20)	784 w	788 (4.8)	Ring
771 s	773 (1.1)			Ring
711 s	694 (17)	711 m	702 (11)	Ring
618 s	620 (4.2)			δ (C=N–C)
511 w	521 (6.5)	508 vw	502 (2.3)	C–O–C + Ring
477 s	483 (6.8)	477 m	481 (2.61)	Ring (C–H)
438 s	417 (1.3)	438 w	429 (6)	Ring
		310 m	300 (53)	ν_{as} Hg–Cl_2
		296 m		ν_{as} Hg···Cl_2
		271 m	262 (13)	ν_s Hg–Cl_2
		260 m		ν_s Hg···Cl_2
		113 m	112 (0.88)	ν Hg–N
		84 m	84 (23)	δ Hg–Cl_2

to the fact that the oxygen atom is involved in an intermolecular hydrogen bond (see Tables 3 and 4).

The vibrations of the Hg–Cl and Hg–N bonds are observed below 400 cm^{-1}. For that reason, the far infrared and Raman spectra were also investigated. The two bands observed at 310 and 296 cm^{-1} in the far infrared spectrum were assigned to the asymmetric stretching of the different Hg–Cl interactions (Cl1–Hg–Cl2 and $Cl1^{iii}$–Hg–$Cl2^{ii}$). In addition, the bands at 271 and 260 cm^{-1} were assigned to the symmetric modes of these groups, and in the Raman spectrum they were observed as a strong band and a shoulder at 271 and 263 cm^{-1}, respectively. These bands are absent in the ligand spectrum. The Hg–N bond is confirmed by the band at 113 cm^{-1} according to DFT results.

3.3 Electronic absorption spectrum

Figure 4 shows the electronic absorption spectrum of an ethanolic solution of the complex. The compound absorbs in the 190–380 nm range, and in comparison with the ligand spectrum, the bands are assigned to π–$\pi^\star$ transitions [23]. The molar absorption coefficients ε have been determined in ethanol with values of 35 500 and 4500 M^{-1} cm^{-1} at 226 and 330 nm, respectively. No d–d transitions were observed in the spectrum of the complex as expected for d^{10} Hg(II) complexes.

3.4 Luminescence properties

The photoluminescence of the complex was measured in aqueous solution (~10^{-4} M) in the 335–600 nm range (Fig. 4). The emission spectrum of the free ligand exhibits two bands due to the existence of an acid–base equilibrium, as previously reported [24]. In this way, the band due to the protonated species is observed at 430 nm and that of the non-protonated one at 363 nm upon excitation with light of 300 nm [25]. The spectrum of the complex shows a very strong emission in the 340–550 nm spectral

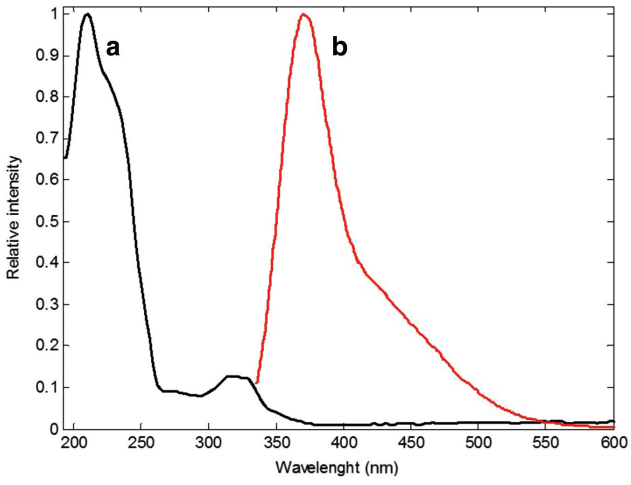

Fig. 4: Normalized UV/Vis (a) and emission (b) spectra of $Hg(6MQ)Cl_2$ at room temperature in aqueous ethanolic solution.

range, with a band centered at 370 nm and a shoulder in the violet-blue region close to 430 nm upon excitation at 325 nm. The band close to 430 nm is decreased in its intensity upon complexation. This fact could be explained taking into account that the quinolinic nitrogen is bonded to the Hg(II) center, and for that reason the acid–base equilibrium is forbidden. The bands observed in the emission spectrum of the complex were assigned to the π–π^* intraligand fluorescence [24, 25].

3.5 Photochemical activity towards singlet oxygen production

The quantum yield of molecular singlet oxygen O_2 ($^1\Delta_g$) production Φ_Δ is defined as the number of photosensitized O_2 ($^1\Delta_g$) molecules per absorbed photon. This property is an indicator of the capacity of a substrate to generate singlet oxygen mainly from its triplet state [26]. Herein the singlet oxygen was indirectly detected by measuring the consumption rate of 9,10-dimethylanthracene (DMA) by irreversible photooxygenation. Bengal Rose (BR) was used as reference photosensitizer (Φ_Δ = 0.68) [26]. The measurements were carried out three times at constant temperature of 25 °C.

$$\Phi_\Delta^{[\mathrm{Hg(6MQ)Cl_2}]} = \Phi_\Delta^{\mathrm{BR}} \frac{k^{[\mathrm{Hg(6MQ)Cl_2}]}}{k^{\mathrm{BR}}} \quad (1)$$

The first-order kinetic constants for the consumption of DMA by the $^1O_2$ generated in the photosensitization with BR and $Hg(6MQ)Cl_2$ as photosensitizers were calculated, giving values of 4.67×10^{-3} and 2.76×10^{-3} s^{-1}, respectively. The quantum yield of singlet oxygen generation of the complex is 0.48 ± 0.07, according to Eq. (1). Although this value is lower than that of the free ligand (0.96 ± 0.08), the complex is probably good enough to be used as photosensitizer in AOP where values of Φ_Δ lower than 0.5 were reported [27]. This value is similar to that of widely known photosensitizers such as methylene blue (0.50), benzophenone (<0.50) and complexes of phthalocyanine with Mg(II) (0.40) and Zn(II) (0.40) [26].

3.6 Thermogravimetric study of the complex

The TG curve of the complex shows the total decomposition in only one step. The weight loss starts at nearly 110 °C and ends at around 350 °C. The relatively high temperature of the thermal decomposition of the mercury complex suggests the possibility of using it in AOP.

4 Conclusions

The crystal structure of a mercury(II) complex with 6MQ is reported for the first time. Different hydrogen bonding and $\pi\cdots\pi$ slipped stacking interactions stabilize the crystal structure. The complex exhibits a very strong luminescence. A relatively high quantum yield of singlet oxygen production was found indicating that the complex could be used in photosensitizing processes. The structural data derived from FTIR and Raman spectroscopies are in a good agreement with those determined by X-ray diffraction and DFT results.

Acknowledgments: The authors would like to thank Universidad Nacional de Colombia (DIME 20101008123), COLCIENCIAS of Colombia, Universidad Nacional de La Plata, CONICET (PIP 356 and PIP 1529) and ANPCyT (PME06 2804 and PICT06 2315) of Argentina for providing financial support.

References

[1] G. G. Aloisi, A. Barbafina, M. Canton, F. Dall'Acqua, F. Elisei, L. Facciolo, L. Latterini, G. Viola, *Photochem. Photobiol.* **2004**, *79*, 248.
[2] A. G. Motten, L. J. Martínez, N. Holt, R. H. Sik, K. Reszka, C. F. Chignell, H. H. Tonnesen, J. E. Roberts, *Photochem. Photobiol.* **1999**, *69*, 282.
[3] C. Valencia, Dissertation, Universidad de Chile, Santiago de Chile (Chile) **2003**.
[4] M. I Litter in *Environmental Photochemistry*, Part II, (Eds.: P. Boule, D. W. Bahnemann, P. K. J. Robertson), Springer-Verlag, Berlin, Heidelberg, **2005**, chapter 2.2, p. 332.
[5] J. R. Allan, J. Dalrymple, *Thermochim. Acta* **1991**, *191*, 223.
[6] F. Zahir, S. J. Rizwi, S. K. Haq, R. H. Khan, *Environ. Toxicol. Pharmacol.* **2005**, *20*, 351.
[7] CrysAlisPro Software System, Intelligent Data Collection and Processing Software for Small Molecule and Protein Crystallography, Agilent Technologies Ltd., Yarnton, Oxfordshire (U. K.) **2013**.
[8] G. M. Sheldrick, Shelxs-97, Program for the Solution of Crystal Structures, University of Göttingen, Göttingen (Germany) **1997**.
[9] G. M. Sheldrick, *Acta Crystallogr.* **1990**, *A46*, 467.
[10] G. M. Sheldrick, Shelxl-97, Program for the Refinement of Crystal Structures, University of Göttingen, Göttingen (Germany) **1997**.
[11] M. J. Frisch, G. W. Trucks, H. B. Schlegel, G. E. Scuseria, M. A. Robb, J. R. Cheeseman, J. A. Montgomery, Jr., T. Vreven, K. N. Kudin, J. C. Burant, J. M. Millam, S. S. Iyengar, J. Tomasi, V. Barone, B. Mennucci, M. Cossi, G. Scalmani, N. Rega, G. A. Petersson, H. Nakatsuji, M. Hada, M. Ehara, K. Toyota, R. Fukuda, J. Hasegawa, M. Ishida, T. Nakajima, Y. Honda, O. Kitao, H. Nakai, M. Klene, X. Li, J. E. Knox,

H. P. Hratchian, J. B. Cross, V. Bakken, C. Adamo, J. Jaramillo, R. Gomperts, R. E. Stratmann, O. Yazyev, A. J. Austin, R. Cammi, C. Pomelli, J. W. Ochterski, P. Y. Ayala, K. Morokuma, G. A. Voth, P. Salvador, J. J. Dannenberg, V. G. Zakrzewski, S. Dapprich, A. D. Daniels, M. C. Strain, O. Farkas, D. K. Malick, A. D. Rabuck, K. Raghavachari, J. B. Foresman, J. V. Ortiz, Q. Cui, A. G. Baboul, S. Clifford, J. Cioslowski, B. B. Stefanov, G. Liu, A. Liashenko, P. Piskorz, I. Komaromi, R. L. Martin, D. J. Fox, T. Keith, M. A. Al-Laham, C. Y. Peng, A. Nanayakkara, M. Challacombe, P. M. W. Gill, B. Johnson, W. Chen, M. W. Wong, C. Gonzalez, J. A. Pople, GAUSSIAN 03 (revision D.01), Gaussian, Inc., Wallingford CT (USA) **2004**.

[12] A. D. Becke, *J. Chem. Phys.* **1993**, *98*, 5648.

[13] P. C. Hariharan, J. A. Pople, *Theor. Chim. Acta.* **1973**, *28*, 213.

[14] W. R. Wadt, P. J. Hay, *J. Chem. Phys.* **1985**, *82*, 284.

[15] P. J. Hay, W. R. Wadt, *J. Chem. Phys.* **1985**, *82*, 299.

[16] P. J. Hay, W. R. Wadt, *J. Chem. Phys.* **1985**, *82*, 270.

[17] J. Wu, H. Hsu, C. Chan, Y. Wen, C. Tsai, K. Lu, *Cryst. Growth Des.* **2009**, *9*, 258.

[18] Ž. Soldin, D. Matković-Čalogović, G. Pavlović, J. Popović, M. Vinković, D. Vikić-Topić, Z. Popović, *Polyhedron* **2009**, *28*, 2735.

[19] M. Kalyanasundari, K. Panchanatheswaran, W. T. Robinson, H. Wen, *J. Organomet. Chem.* **1995**, *491*, 103.

[20] P. Pyykkö, M. Straka, *Phys. Chem. Chem. Phys*. **2000**, *2*, 2489.

[21] C. Janiak, *J. Chem. Soc., Dalton Trans*. **2000**, *21*, 3885.

[22] K. J. Wei, J. Ni, Y. S. Xie, Q. L. Liu, *Inorg. Chem. Commun.* **2007**, *10*, 279.

[23] Y. T. Varma, S. Joshi, D. D. Pant, *AIP Conference Proceedings*, **2013**, *1536*, 1123.

[24] L. R. Naik, H. M. Suresh Kumar, S. R. Inamdar, N. N. Math, *Spectrosc. Lett.* **2005**, *38*, 645.

[25] T. Ikeyama, T. Azumi, T. Murao, I. Yamazaki, *Chem. Phys. Lett.* **1983**, *96*, 419.

[26] F. Wilkinson, W. P. Helman, A. B. Ross, *J. Phys. Chem. Ref. Data* **1993**, *22*, 113.

[27] M. E. Jiménez-Hernández, F. Manjón, D. García-Fresnadillo, G. Orellana, *Sol. Energy* **2006**, *80*, 1382.

Graphical synopsis

Cristian Villa-Pérez, Isabel C. Ortega, Angélica M. Payán-Aristizábal, Gustavo Echeverría, Gloria C. Valencia-Uribe and Delia B. Soria

Synthesis, crystal structure and physicochemical characterization of a Hg(II) complex with 6-methoxyquinoline as ligand

DOI 10.1515/znb-2015-0069
Z. Naturforsch. 2015; x(x)b: xxx–xxx